Published in final edited form as:
Neuroimage. 2012 August 15; 62(2): 1241–1248. doi:10.1016/j.neuroimage.2011.10.065.

The future of ultra-high field MRI and fMRI for study of the human brain

Jeff H. Duyn*
Advanced MRI Section, Laboratory of Functional and Molecular Imaging, National Institute of Neurological Disorders and Stroke, National Institutes of Health, Building 10 Room B1D724, 9000 Rockville Pike, Bethesda, Maryland, USA

Abstract

MRI and fMRI have been used for about three and two decades respectively and much has changed over this time period, both in the quality of the data and in the range of applications for studying the brain. Apart from resolution improvements from around 4 mm in the early days to below 0.5 mm with modern technology, novel uses of contrast have led to the ability to sensitize images to some of the brain's structural properties at the cellular scale as well as study the localization and organization of brain function at the level of cortical columns. These developments have in part been facilitated by a continuing drive to increase the magnetic field strength. Will the next few decades see similar improvements? Here we will discuss current state of high field MRI, expected further increases in field strength, and improvements expected with these increases.

Keywords

High field MRI; Magnet technology; RF coils; Resolution; Contrast; Brain function; Brain structure; Myelin; Cortex

Introduction

Scientific discoveries and technological advancements often go hand in hand. A prominent example of this relationship is the discovery of X-rays and its subsequent use in crystallography, leading to the discovery of the structure of DNA and the development of modern molecular genetics and the CT-scanner. Similarly, in optics, lens optimization in the early microscopes led to the discovery of red blood cells and bacteria, and the development of optical techniques such as photo-activated localization microscopy (PALM) and fluorescence resonance energy transfer (FRET) has revolutionized cell biology.

Technological advances in a number of fields have also made a significant impact in the field of neuroscience. MRI is an excellent example of this, as it has, since its initial introduction in the clinic in the late seventies and early eighties, rapidly become the main modality not only for clinical neuroimaging, but also for basic research into the structure and function of the human brain.

Like with other brain imaging techniques such as positron emission tomography and CT, MRI has experienced a number of major developments since its early years, and as a result the quality and breadth of applications has increased tremendously. One important

*Fax: +1 301 480 1981. jhd@helix.nih.gov.

technological development that has continued over the entire lifespan of MRI is the increase in magnetic field strength, made possible by improvements in design and technology of the magnet; in parallel, associated radio-frequency (RF) electronics and magnetic field gradients have continuously improved, facilitating the practical use of high field strength MRI systems. These field strength increases have improved the study of both the brain's function and structure, as they provide for increases in sensitivity, contrast, and resolution.

For example, the early work leading up to the invention of fMRI two decades ago was greatly facilitated by the availability of magnets with fields substantially higher than the 1.5 T operating field of conventional clinical systems. Thulborn's early work on the dependence of transverse dipolar (T_2) relaxation on blood oxygenation in cannulated blood vessels in rodents benefited from an increased contrast available at the relatively strong field of 4.3 T (Thulborn et al., 1981). Ogawa's early work on T_2^* (a combination of dipolar and magnetic susceptibility effects) relaxation dependence on blood oxygenation in rat brain was performed at 7 T (Ogawa and Lee, 1990; Ogawa et al., 1990), and his group's early human fMRI work based on BOLD contrast was performed at 4 T (Ogawa et al., 1992). An additional enabling technology in the early development of fMRI was rapid gradient switching that made rapid scanning techniques such as echo planar imaging (EPI) possible (Bandettini et al., 1992; Kwong et al., 1992; Turner et al., 1993). In large part because of the increased magnetic susceptibility contrast at high field that underlies the BOLD effect, many of the major fMRI research sites now own 7 T human scanners. These systems allow fMRI with increased sensitivity, specificity, and resolution compared to their lower field predecessors (Triantafyllou et al., 2005; Yacoub et al., 2008; Uludag et al., 2009).

Structural MRI has also benefitted from the increased resolution and contrast available at high magnetic fields. For example, the better resolution achieved when going from 1.5 T to 3 T has improved the separation of gray and white matter, and enabled quantification of cortical volume, an important parameter for the longitudinal monitoring of disease progression. At fields ranging from 7 T to 9.4 T, magnetic susceptibility-weighted techniques have allowed improved visualization of small anatomical structures based on susceptibility differences between blood, iron, and myelin (Bourekas et al., 1999; Christoforidis et al., 1999; Li et al., 2006; Duyn et al., 2007; Cho et al., 2010; Budde et al., 2011). In the CNS, white matter fibers, vascular structures, and the layer structure of cortical gray matter are being revealed at resolutions of several 100's of microns (Duyn et al., 2007; Kang et al., 2010; Marques et al., 2010). The combination of such data with high resolution functional data available with high field fMRI offers unique opportunities for the study of the relationship between structure and function in the human brain.

Given these important advantages of high field MRI for the non-invasive study of the human brain, it is natural to ask the question, where does the push for high field lead to and where will it end? As is the case in many research fields, cutting-edge technology comes at a price. With MRI, this price is increased system complexity and cost, and possibly reduced versatility. The latter may mean some applications may have limited benefit from high field or not be possible on the highest field systems, due to limited bore size (on a head-only system) or other restrictions. Is this price outweighed by the expected improvements? Will high field MRI find widespread application and be used clinically? In this review, we will look at some of these issues with a focus on applications to the study of human brain.

Where are we now

Over its relatively short (3 decades) existence, MRI has become the imaging technique of choice for the study and clinical evaluation of the brain and spine. Major applications include stroke and trauma, vascular abnormalities, spinal cord compression, primary and

metastatic brain tumors, brain infection, and Multiple Sclerosis (MS). MRI has important applications outside the nervous system as well, most notably in organs such as the heart, breast, pelvic organs and in the muskoskeletal system. Worldwide, more than 60 million clinical MRI scans are performed annually on over 25,000 MRI systems. Interestingly, most of these systems are used purely for clinical purposes and operate at low field at or below 1.5 T, while only a small fraction (5–10%) is at field strengths of 3 T or above. One reason for this is the increased cost of higher field systems, which in a number of established clinical applications (particularly outside the brain) may not be justified by the expected benefits. Furthermore, the effect of field strength on clinical diagnosis requires is often difficult to quantify and its proper evaluation requires well controlled comparative studies.

Nevertheless, at major neuroimaging centers of hospitals and universities, the fraction of systems that operates at 3 T is substantially higher, and a number of institutions are using or planning to use even higher field strength systems. For example, there are currently about thirty-five 7 T systems that are being used primarily for research applications, and this number is steadily growing. There are also research 9.4 T systems being used at universities in Chicago, Minnesota, Juelich (Germany), and Tuebingen (Germany). Even higher field systems at 10.5 T, 11.7 T and 14 T are being installed or are in the planning stages in Minnesota, NIH, Saclay (France), and in Korea. The primary goal of these highest field systems is to explore the boundaries of neuroimaging in order to obtain structural and functional information with the highest possible spatial resolution, with the hope that this may lead to novel scientific and clinical discoveries.

What to expect from higher field

Historically, with each step increase in magnetic field strength, we have seen altered sensitivity and contrast, and improved spatial resolution, which have led to new structural and functional information and which have broadened MRI's possible applications. Is this going to continue in the coming decades? In the following, we will discuss what we expect will happen to resolution, sensitivity, and contrast with further increases in field strength.

Spatial resolution improvement

The human brain is a highly heterogeneous organ with structural and functional complexities at various spatial scales. The ability for an imaging technique to fully resolve these complexities is in part dependent on its spatial resolution. For most anatomical scans on clinical scanners operating at 3 T, and employing modern detectors (i.e. receive coils), the spatial resolution is around $1\times1\times1$ mm^3, which is equivalent to 1 μl volume for each spatially resolved element or "voxel". For 3 T functional scans based on BOLD or perfusion contrast, the spatial resolution is somewhat inferior and generally limited to about $2\times2\times2$ mm^3 due to the fact that the effect size (i.e. temporal or spatial contrast) is only a few percent of the available signal. The use of higher resolutions generally reduces both image signal-to-noise ratio (SNR) and contrast-to-noise ratio (CNR), and image noise starts to overwhelm the anatomical or functional detail. In contrast, modern 7 T scanners allow improvement of the fMRI resolution to about $1\times1\times1$ mm^3, and of some anatomical applications to $0.5\times0.5\times0.5$ mm^3. This improvement is possible in part because of the increases of SNR and CNR with field strength, and in part because of the reduced partial volume effects for certain applications. As a result, high field MRI is starting to allow the detection of features that are well within the dimensions of the cortical ribbon, an important target for functional and morphometric studies.

How much further can resolution be improved with further increases in field strength? Can we expect to ultimately be able to reach resolutions of a few microns and image single neurons, as has been demonstrated on NMR microscopy systems operating at 14 T (Weiger

et al., 2008; Flint et al., 2009)? Barring spectacular new developments, the answer is: "probably not". NMR microscopy experiments have a number of advantages (other than the higher field strengths available for the small-bore magnets they use) that do not apply to scanning human brain in-vivo, including the use of very small (sub-millimeter) objects, scan times of many hours without object motion, and imaging gradients that are orders of magnitude stronger than human-scale gradients. The object size in particular can have quite substantial effects on attainable resolution. For example, with appropriately sized coil detectors that contribute minimally to the noise, SNR for an object that is n times smaller in each dimension is roughly $n^{2.5}$ times improved (see e.g. (Macovski, 1996)), meaning that, because image SNR scales with voxel volume, the resolution can be increased by almost n-fold in each dimension. In contrast, the resolution improvement available when the field strength increases by a factor n has a smaller effect on the resolution of approximately $1/n^{0.33}$, assuming that SNR increases linearly with field strength (Redpath, 1998). It appears therefore that improvement of the resolution in structural MRI of the human brain to below 200 μm will require major improvements in detector and gradient design in addition to increased field strength.

Over the past decade, there have been significant improvements in detector sensitivity. Using array detectors, the object under study can be figuratively subdivided in many small objects by using a detector with a large number of small elements that are placed around the head. In particular in superficial brain areas close to these coils, sizable SNR improvements have been obtained reaching factors of 3–10 compared to volume coils (Porter et al., 1998; de Zwart et al., 2002a, 2004; Wiggins et al., 2006, 2009) at clinical field strengths (1.5–3 T), and these improvements are expected to be even higher at higher fields. This latter is in part because the reduced (relative) contribution of coil and amplifier noise at high field allows smaller (and thus more) elements to be used without compromising SNR in areas away from the brain's surface. A practical limit of this size reduction is when the diameter of the coil approaches the distance between coil and brain tissue, beyond which no significant further gains are obtained even in tissue closest to the coil. Under most conditions, this distance is at least 1–2 cm due to physical and safety constraints. It is important to keep in mind however that the actual SNR improvement achieved with array coils at high field is also dependent on the geometry and size of the object, as wavelength effects at high field may locally increase or decrease SNR (Ocali and Atalar, 1998).

In addition to the synergistic effect of high field and array performance on SNR, additional improvements may come from new ways to detect magnetic fields, several of which have been developed over recent years for small-scale applications. Examples are diamond magnetometers to detect single spins (Balasubramanian et al., 2008; Maze et al., 2008), and alkali-metal magnetometers (Kominis et al., 2003). It remains to be seen if any future developments in the way we detect magnetic fields field will translate to human imaging.

Others factor that may limit spatial resolution in human applications are brain and head motion, and blurring caused by magnetic susceptibility effects. The former can be particularly problematic due to the increased scan times and lower tolerance to motion associated with high resolution MRI. While correction strategies based on MRI navigator signals or external tracking devices (see e.g. (Ward et al., 2000) and (Qin et al., 2009)) may be able to largely resolve the effects of rigid head motion, they will be less effective in correcting for incoherent (non-rigid) displacements associated with brain pulsation, which may reach around 100 μm in some brain regions (Soellinger et al., 2009). Timing (i.e. gating) the MRI pulse sequence with the respiratory and cardiac cycles may be necessary when imaging at such resolutions.

Changes in contrast with field strength

For MRI of the human brain, intrinsic SNR and resolution increases alone may not justify the increasingly difficult and costly task of raising field strength beyond what is available on current state of the art systems that operate at 7 T or even at 3 T. One of the most interesting phenomena at high field however is the change in contrast in many applications, including spectroscopic techniques and techniques used for functional and structural imaging. This change arises from the fact that the mechanisms underlying the NMR signal generation process depend on field strength, leading to substantial changes in relaxation time constants T_1, T_2 and T_2^*, and in spectral and spatial frequency contrast due to chemical shift and magnetic susceptibility effects. This dependence of contrast on field strength will affect not only the type of things we can see, but also the practical resolution that can be reached.

Some of the most obvious contrast increases with field strength have been observed in structural MRI and BOLD fMRI using T_2^*-weighted gradient echo imaging, which exploits the sensitivity of the NMR signal to variations on the local magnetic field due magnetic susceptibility effects. Susceptibility-weighted techniques have allowed the visualization of features that before were not or only marginally resolved. For example, structural studies using susceptibility contrast at 7 T have allowed robust visualization of laminar structure in several cortical regions including visual and motor cortices and the cerebellum (Duyn et al., 2007; Kang et al., 2010; Marques et al., 2010). Within subcortical structures such as the amygdala and hippocampus and in the substantia nigra, this contrast has allowed their anatomical sub-divisions (Thomas et al., 2008; Cho et al., 2011; Solano-Castiella et al., 2011). In human fMRI, voxel resolutions at or below the cortical thickness have become possible, and are starting to allow the resolution of column and layer specific signals (Yacoub et al., 2008; Polimeni et al., 2010).

These improvements have come from CNR increases resulting from increasing field strength. In addition, some of these observations been facilitated by the reduced partial volume effect associated with smaller voxel sizes. The latter effect depends on the size of the contrast source. For example, contrast from a vessel within an imaging voxel will increase linearly with reduction of the voxel volume, down to the size of the vessel. Combined with the fact intrinsic SNR is linearly dependent on voxel size, the voxel reduction in this example comes without loss in CNR.

Estimation of further CNR improvements in T_2^*-weighted imaging with future increases in field strength requires knowledge of the field dependencies of the relaxation time constants, which for some tissues can be extrapolated from recent work on human brain or deduced from studies of animal brain (Peters et al., 2007; Uludag et al., 2009; Yao et al., 2009; Seehafer et al., 2010; Budde et al., 2011). For example, the field strength dependencies of T_2^* and T_1 relaxation can be heuristically approximated by:

$$R_1 = a + b \cdot B_0^c \quad (1a)$$

$$R_2^* = d + e \cdot B_0 \quad (1b)$$

with $R_1 = 1/T_1$, $R_2^* = 1/T_2^*$, B_0 the static magnetic field strength, and a, b, c, d, and e constants that vary with tissue type (Fig. 1a). Values for these constants in cortical gray matter are approximately 0.35, 0.64, −0.7, 7, and 3.5 respectively when using SI-based units (Grohn et al., 2005; Peters et al., 2007; Uludag et al., 2009). Assuming the MRI repetition time (TR) is well below T_1, and that a constant proportion of the signal decay curve is collected by using a signal acquisition window that starts immediately after excitation and

has a duration that scales with T_2*, the field dependencies of SNR and CNR can be approximated by:

$$SNR \propto B_0 \cdot \sqrt{\frac{R_1}{R_2^*}} \tag{2a}$$

$$CNR \propto B_0 \cdot \sqrt{\frac{R_1}{R_2^*}} \cdot \frac{\Delta R_2^*}{R_2^*}. \tag{2b}$$

These equations are based on optimal scanning conditions (TR< T_1, optimal fiip angle), with the assumption that the noise exclusively originates from resistive (thermal) sources in the sample that has an electrical conductivity independent of field strength. They apply to temporal contrast in BOLD fMRI and spatial contrast in susceptibility weighted structural MRI based on magnitude signal (i.e. signal amplitude), with ΔR_2* in Eq. (2b) representing the temporal or spatial change in R_2*. For frequency contrast (i.e. contrast based on signal phase), the factor ΔR_2* is replaced by a frequency shift Δf. The factor $\sqrt{R_1}$ in the term $\sqrt{R_1}/\sqrt{R_2^*}$ represents increased T_1-saturation at high field, whereas $1/\sqrt{R_2^*}$ represents increased T_2* relaxation and the associated shortening of the signal decay curve.

Substitution of Eqs. (1a) and (1b) into Eq. (2b) indicates that the term $\sqrt{R_1}/\sqrt{R_2^*}$ reduces the SNR gains available with high field systems by an amount that, in the high field limit, approaches $1/\sqrt{B}$. As a result, the overall dependence of SNR on field approaches $\sqrt{B}$ (Fig. 1b). CNR on the other hand has the additional term $\Delta R_2^*/R_2^*$ (or $\Delta f/R_2^*$), which increases with field strength, making CNR increase faster with field than SNR does. Assuming a linear increase of ΔR_2* and Δf with field (Uludag et al., 2009; Yao et al., 2009), the term initially increases with field but levels off above about 10 T (Fig. 1c). As a result, above 10 T the field dependency of CNR also approaches $\sqrt{B}$ (Fig. 1b).

It is important to note that the factor $1/\sqrt{R_2^*}$ representing shortening of the T_2* decay curve is specific to gradient echo MRI and may not or to a lesser extent apply to other applications that mitigate the contribution of susceptibility effects to T_2* decay through RF refocusing, as is done with fast spin echo (FSE), steady state free precession (SSFP) and T_{1rho} (Grohn et al., 2005) techniques. However, at high field, effective refocusing is increasingly more difficult to accomplish due to the stronger susceptibility effects and limits on B_1 (i.e. transmit field) amplitude imposed by safety issues related to tissue heating (see below).

The estimates presented above represent lower limits to the gains in SNR and CNR we can expect with further increases in field strength. Importantly, for BOLD fMRI, a number of studies have suggested that certain vascular compartments may show a more than linear and possibly quadratic increase of ΔR_2* with field strength (Turner et al., 1993; Uludag et al., 2009). In addition, at high field as compared to low field, one may be better able to capture the full T_2* decay curve when scan time is a limiting factor. These effects could increase the dependence of CNR on field, under specific conditions, to B_0 or even B_0^2. The latter may be rather optimistic for BOLD fMRI in general as it may, for example, not apply to spin-echo acquisitions or field increases much beyond 7 T (Uludag et al., 2009; Seehafer et al., 2010).

For structural MRI, CNR improvements allow improved visualization of subtle contrast differences (at constant resolution and scan time), reduced scan time (at constant CNR and

resolution), or improved resolution (at constant CNR and scan time). For fMRI one the other hand, this tradeoff is somewhat more complicated due to the presence of physiological noise sources, which, if not properly characterized and separated from the signal (Bianciardi et al., 2009a, 2009b), limit the improvements in detection sensitivity available with high field MRI (Triantafyllou et al., 2005, 2011).

In addition to increasing CNR and SNR, high field strength systems will facilitate the study of field dependent changes in contrast, which may improve the understanding of the underlying contrast mechanisms, and as a result may enable the extraction of certain types of microstructural and chemical information difficult to access at low field. For example, at high field, the field dependent term of R_2^* in Eq. (1b) becomes dominant in regions such as the basal ganglia, allowing direct inference of their iron content by measuring local R_2^* values (Yao et al., 2009). This may also be possible in cortical gray matter (Fukunaga et al., 2010a). In white matter, the improved contrast at high field may facilitate the detection of multi-exponential T_2^* relaxation, potentially providing information about axonal myelination (Hwang et al., 2010; van Gelderen et al., 2011), and complementing information available from T_2 studies at lower field strength. Similarly, in fMRI, contrasts from vascular compartments such as the capillary bed, principal intra-cortical veins, and pial veins may show differing field dependencies, possibly allowing fMRI signals more specific to the capillary bed and therefore potentially better localized (Ugurbil et al., 1999; Uludag et al., 2009; Donahue et al., 2011).

Other applications that may see substantial benefits from field strength increases are techniques based on magnetization transfer (MT) contrast and spectroscopic techniques used for metabolic studies. Contrast in these techniques is derived from chemical shift effects, which scale linearly with field strength. As a result, MT and spectroscopic contrast is generally increased at high field. Combined with a close to linear increase in SNR with field (assuming an only small contribution of T_2^* effects), this would provide the opportunity for a more than linear increase in CNR. This has been observed for proton spectroscopy when increasing the field strength from 4 T to 7 T (Tkac et al., 2001) and 9.4 T (Deelchand et al., 2010), and for phosphorous spectroscopy going from 4 T to 7 T (Qiao et al., 2006), and this trend is expected to continue at field strengths well above 7 T. An interesting development that combines MT and spectroscopic contrast is the use of chemical exchange saturation transfer to detect brain myo-inositol (Haris et al., 2011).

Of course, in specific situations, other methods to improve the ability to detect small features may be applicable as well, including use of exogenous contrast agents such as paramagnetic (Shapiro et al., 2006) or hyperpolarized (Albert et al., 1994) compounds. In addition, sometimes the desired information about small structural variations in the brain can be obtained without having the image resolution available to spatially resolve those structures. For example, using diffusion-weighted MRI, it is starting to become possible to measure not only fiber orientation, but also axonal size distributions based on the tissues water diffusion characteristics (Barazany et al., 2009). In addition, a recent study suggests that the interaction of diffusion gradients with susceptibility gradients provides and alternative mechanism that allows the measurement of fiber orientation, even in the absence of diffusion anisotropy (Han et al., 2011).

What are apparent field strength limits

Although Eqs. (2a)–(2b) suggest a continued increase in SNR and CNR with increasing field, there are a number of issues that have slowed the adoption of high field systems for clinical use and are limiting the ultimate fields that may be used in future systems. These range from economical issues to technological and physiological/biological limits.

Modern MRI scanners of 1.5 T and above use superconductive magnets for their excellent stability; however these magnets become increasingly more difficult to make due to the fact that current density that can be used in the superconductive wires that generate the magnetic field decreases with field strength. For example, the widely used Niobium–Titanium superconductor has a maximum current density (also called “critical current density”) that drops rapidly with increasing field, limiting its application to fields up to about 12 T. Another difficulty with producing high field magnets comes from the Lorentz forces acting on the conductors, which increase with field strength (and wire current) and put stringent mechanical requirements on the magnet construction and further limit critical current density.

At fields higher than 12 T, other wire types are required, which may be more expensive to produce or more difficult to work with. For example, the much more expensive Niobium–Tin wire has been used (generally in combination with Niobium–Titanium) to produce small bore systems for animal MRI and structural NMR analysis of small samples, with fields up to 23 T. Alternatively, fields higher than 12 T could be generated by a combination of superconductive and resistive conductors, however, such systems will likely have poorer stability. Practical human-size MRI systems at fields much beyond 12 T will therefore likely require the use of low cost superconductors with much improved current densities.

Another limit of high field MRI relates to the radio-frequency (RF) electro-magnetic transmission and reception fields that are used for signal generation. At the higher RF frequencies used in high field systems, the interaction of RF fields with the object and the environment is altered, and this has significant practical applications. First of all, RF wavelength effects in the object lead to non-uniform transmit fields, leading to spatial variations in SNR and CNR. Some of these effects can be mitigated by sophisticated scan techniques, however, these have limits and at fields of 12 T and above, they will likely leave substantial brain areas with suboptimal SNR and contrast. Secondly, at higher frequencies, it becomes more difficult to control electro-magnetic coupling between the various elements in the transmit and receive structures, and between these elements and the environment (i.e. radiation losses). Third, the RF power required for an imaging experiment increases with field strength, resulting in increased tissue heating and limiting the range of experiments that can be performed in humans (see below). Lastly, non-uniformities in B_1 and B_0 due to wavelength effects and magnetic susceptibility effect respectively can lead to an increased level of image artifacts at high field. In summary, RF issues substantially complicate the practical use of high field MRI and make it increasingly more difficult to attain the theoretically predicted gains (i.e. Eqs. (2a)–(2b)) over large areas of the brain.

There are also physiological issues that limit the field strengths attainable for human MRI, the most important of which are caused by movement in the B_0 field, and tissue heating caused by RF power deposition. Movement in a static field may affect some of the sensory afferents of the central nervous system and can lead to temporary experiences such as a metallic taste (Cavin et al., 2007), magneto-phosphenes (Barlow et al., 1947), or vertigo and nausea (Glover et al., 2007). Such effects are starting to become apparent in some persons under certain conditions at 7 T and 9.4 T, and are expected become more common at higher fields. They can be substantially reduced by minimizing head motion in the proximity of or inside the magnet. There are currently no indications that exposure of living beings to static magnetic field itself is harmful at any field strength.

RF tissue heating may be more limiting to the ultimate field strength that one can safely use for human MRI. Tissue heating results from the time-varying electrical fields associated with RF transmission and increases approximately quadratically with B_0 for a given electrical field strength. Furthermore, stronger spatial variations in electrical fields at high

B_0 due to wavelength effects may cause locally elevated heating. At 7 T this is starting to become problematic as the heating associated with some of the popular scan techniques starts to approach the safety limit of 1 °C. Optimization of RF transmit coils and excitation pulses may alleviate this problem to some extent. Another approach is to avoid certain scan techniques, or adjust the parameters of the scan to minimize the heating effects. Nevertheless, at fields of 7 T and above, RF-induced tissue heating increasingly forces practical trade-offs that reduce the breadth of available applications and may ultimately affect SNR and CNR.

Future potential of high 3eld MRI and adoption for clinical use

High field MRI with field strengths up to 9.4 T in humans and close to 20 T in animals has already impacted basic sciences and this impact is expected to grow with the increased availability of high field systems. In rodents, isotropic resolutions of 350 Mμ and 75 Mμ for functional and structural have been achieved, benefiting from the fact that intrinsic sensitivity increases about linearly with reductions in brain volume (V). Combined with the fact that in small mammals, important structural dimensions such as cortical and laminar thickness are only reduced by $V^{0.1}$ (Zhang and Sejnowski, 2000), this has allowed the study of fMRI activity and neurovascular coupling at the laminar and columnar scale (Kim et al., 2000; Duong et al., 2001; Silva and Koretsky, 2002; Kim and Kim, 2010; Yu et al., 2011).

Structural MRI at 3 T and above is starting to reveal the contributions to magnetic susceptibility contrast (He and Yablonskiy, 2009; Lee et al., 2009; Li et al., 2009; Marques et al., 2009; Fukunaga et al., 2010a; Lee et al., 2010; Liu, 2010; Petridou et al., 2010; Langkammer et al., 2011; Li et al., 2011; Liu et al., 2011a; Sati et al., 2011; van Gelderen et al., in press), allowing novel ways to probe tissue microstructure (Lee et al., 2011; Liu et al., 2011b) and may soon allow the mapping of important biological compounds such as iron and myelin in human brain (Fukunaga et al., 2010b; Schweser et al., 2011). Increasing the field strength beyond 7 T and 9.4 T is expected to greatly facilitate such studies, and further is hoped to lead to novel uses and applications of MRI contrast.

For fMRI, potential sensitivity increases with field strength may often be limited due to the presence of physiological noise sources, which generally cause signal fiuctuations that scale with absolute signal strength (Hyde et al., 2001; Kruger and Glover, 2001; de Zwart et al., 2002b). Recent developments in the characterization of these sources (Triantafyllou et al., 2005; Birn et al., 2006; Fox et al., 2007; Shmueli et al., 2007; de Zwart et al., 2008) may reduce the severity of this limitation and therefore allow one to better exploit the increase in SNR and CNR of high field systems. This may be particularly advantageous for the rapidly growing field of deducing brain connectivity from spontaneous neural activity (Fox and Raichle, 2007).

As has been the case throughout the development of MRI, the full benefits of further increases in field will depend on future developments in gradient and RF technology, and pulse sequences for the generation of contrast, the reduction of tissue heating, and the mitigation of artifacts due to non-uniformities in B_0 and B_1. Currently, significant advances are being made in the development of multi-channel RF transmission (to improve B_1 uniformity and reduce tissue heating), pulse sequences to mitigate the effects of non-uniform B_1, and head-only gradient and B_0 shim coils to overcome the increased susceptibility-related signal loss and image distortions at high field and allow the increased scan speed necessary to acquire the large data matrices required for high resolution MRI.

Will high field systems have as much impact on clinical MRI as it is starting to have on basic science research? As indicated above, currently clinical imaging is primarily performed on systems with fields below 3 T primarily because of their lower costs and the

fact that the necessity or even benefit of higher fields for currently common applications has not been demonstrated yet. On the other hand, the improved visualization of fine anatomical structures possible with modern 7 T systems suggests the widespread clinical use of such systems is just a matter of time. In fact, the prospect of a significant clinical role for 7 T MRI of the brain is steadily growing, based on the success of preliminary studies of diseases such as multiple sclerosis (MS) (Ge et al., 2008; Kollia et al., 2009; Tallantyre et al., 2010), Alzheimer's disease (Kerchner et al., 2010), epilepsy (Madan and Grant, 2009; Henry et al., 2011), and movement disorders (Abosch et al., 2010), where 7 T facilitates the detection of anatomical and morphological features and abnormalities. For example in MS, an important advantage of high field MRI may be the improved detection sensitivity of small lesions in the cortex and white matter, and a potentially improved characterization of lesions in general (Ge et al., 2008; Kollia et al., 2009; Tallantyre et al., 2010). In epilepsy, MRI at 7 T has allowed localizing the seizure focus to small cortical regions with dysplasia, greatly facilitating surgical intervention (Madan and Grant, 2009). Similarly, in movement disorders, 7 T MRI allows improved delineation of basal ganglia regions to be targeted with deep brain stimulation using intracortical electrodes (Abosch et al., 2010). Other areas where 7 T is likely to make an impact include angiography and spectroscopy, both of which benefit substantially from improved sensitivity and contrast. High field angiographic MRI studies allow resolutions that compete with those of CT (about 0.4 mm in-plane), without the use of contrast agents or ionizing radiation (Deistung et al., 2008; Kang et al., 2010). In addition, the strong susceptibility effect of deoxyhemoglobin, allows MRI to distinguish between arteries and veins. Neurotransmitter levels of GABA and glutamate, the detection of which is greatly facilitated with modern spectroscopic techniques at high field, affect neuronal excitability and their measurement may provide important information about normal brain function (Muthukumaraswamy et al., 2009; Sumner et al., 2010) as well as diseases such as epilepsy (Wong et al., 2003), schizophrenia (Lewis and Hashimoto, 2007; Marenco et al., 2010), and depression (Sanacora et al., 1999). Similarly, high field may allow the robust measurement of ATP synthesis in order to study diseases with abnormal brain energy metabolism, including the characterization of brain tumors (Beloueche-Babari et al., 2010).

Although the cost of MRI at high field strength such as 7 T is coming down due to more compact electronics and the availability of self-shielded magnets that allow more compact siting and do not require a costly passive iron shield, there are other limitations that are restricting widespread clinical application. The most important of these is that high field systems currently have a narrower operating window due to the fact that a number of applications that run well at low field are susceptibility to artifacts and may generate excessive tissue heating at high field, forcing trade-offs that affect SNR and CNR. These issues are currently subject of active research and it is anticipated that novel pulse sequences and optimized parameters will, to a large extent, eliminate these limitations. It is less likely that this will also be the case for fields as high as 12 and 14 T, which may therefore serve a narrower range of applications. On the other hand, the hope is that the unique contrast of MRI at these field strengths will lead to novel applications.

Summary

The development of high field MRI systems and associated technology has led to novel applications of contrast, which in their turn have motivated further increases in field strength. As a result, MRI has become a powerful technique to look at structural and functional details of the brain at millimeter and sub-millimeter resolution, further broadening its impact on basic neuroscience and clinical research. In the near future, systems of 12 T and possibly even 14 T will become available, offering the prospect of the ability to visualize new features in the brain. Currently, field increases beyond these levels appear prohibitively difficult due to physical, technological and physiological limitations.

Because MRI is such a versatile technique with much possibility to manipulate image contrast, it is difficult to predict the full scope of research and clinical applications that will be available with high field systems in the coming decades. It is nevertheless clear that applications that will see large benefits from continued increases in field strength include structural and functional studies based on magnetic susceptibility contrast, and studies of the effect of tissue energetics and neurotransmitter levels on brain function.

Acknowledgments

Alan Koretsky and Peter van Gelderen of the Laboratory of Functional and Molecular imaging at NIH are acknowledged for helpful discussions and suggestions. This research was supported by the Intramural Research Program of the National Institute of Neurological Disorders and Stroke, National Institutes of Health.

References

Abosch A, Yacoub E, Ugurbil K, Harel N. An assessment of current brain targets for deep brain stimulation surgery with susceptibility-weighted imaging at 7 Tesla. Neurosurgery. 2010; 67:1745–1756. (discussion 1756). [PubMed: 21107206]

Albert MS, Cates GD, Driehuys B, Happer W, Saam B, Springer CS Jr, Wishnia A. Biological magnetic resonance imaging using laser-polarized 129Xe. Nature. 1994; 370:199–201. [PubMed: 8028666]

Balasubramanian G, Chan IY, Kolesov R, Al-Hmoud M, Tisler J, Shin C, Kim C, Wojcik A, Hemmer PR, Krueger A, Hanke T, Leitenstorfer A, Bratschitsch R, Jelezko F, Wrachtrup J. Nanoscale imaging magnetometry with diamond spins under ambient conditions. Nature. 2008; 455:648–651. [PubMed: 18833276]

Bandettini PA, Wong EC, Hinks RS, Tikofsky RS, Hyde JS. Time course EPI of human brain function during task activation. Magn Reson Med. 1992; 25:390–397. [PubMed: 1614324]

Barazany D, Basser PJ, Assaf Y. In vivo measurement of axon diameter distribution in the corpus callosum of rat brain. Brain. 2009; 132:1210–1220. [PubMed: 19403788]

Barlow HB, Kohn HI, Walsh EG. Visual sensations aroused by magnetic fields. Am J Physiol. 1947; 148:372–375. [PubMed: 20284558]

Beloueche-Babari M, Chung YL, Al-Saffar NMS, Falck-Miniotis M, Leach MO. Metabolic assessment of the action of targeted cancer therapeutics using magnetic resonance spectroscopy. Br J Cancer. 2010; 102:1–7. [PubMed: 19935796]

Bianciardi M, Fukunaga M, van Gelderen P, Horovitz SG, de Zwart JA, Shmueli K, Duyn JH. Sources of functional magnetic resonance imaging signal fluctuations in the human brain at rest: a 7 T study. Magn Reson Imaging. 2009a; 27:1019–1029. [PubMed: 19375260]

Bianciardi M, van Gelderen P, Duyn JH, Fukunaga M, de Zwart JA. Making the most of fMRI at 7 T by suppressing spontaneous signal fluctuations. Neuro-Image. 2009b; 44:448–454. [PubMed: 18835582]

Birn RM, Diamond JB, Smith MA, Bandettini PA. Separating respiratory-variation-related fluctuations from neuronal-activity-related fluctuations in fMRI. NeuroImage. 2006; 31:1536–1548. [PubMed: 16632379]

Bourekas EC, Christoforidis GA, Abduljalil AM, Kangarlu A, Chakeres DW, Spigos DG, Robitaille PM. High resolution MRI of the deep gray nuclei at 8 Tesla. J Comput Assist Tomogr. 1999; 23:867–874. [PubMed: 10589560]

Budde J, Shajan G, Hoffmann J, Ugurbil K, Pohmann R. Human imaging at 9.4 T using T(2) *-, phase-, and susceptibility-weighted contrast. Magn Reson Med. 2011; 65:544–550. [PubMed: 20872858]

Cavin ID, Glover PM, Bowtell RW, Gowland PA. Thresholds for perceiving metallic taste at high magnetic field. J Magn Reson Imaging. 2007; 26:1357–1361. [PubMed: 17969179]

Cho ZH, Min HK, Oh SH, Han JY, Park CW, Chi JG, Kim YB, Paek SH, Lozano AM, Lee KH. Direct visualization of deep brain stimulation targets in Parkinson disease with the use of 7-tesla magnetic resonance imaging. J Neurosurg. 2010; 113:639–647. [PubMed: 20380532]

Cho ZH, Oh SH, Kim JM, Park SY, Kwon DH, Jeong HJ, Kim YB, Chi JG, Park CW, Huston J III, Lee KH, Jeon BS. Direct visualization of Parkinson's disease by in vivo human brain imaging using 7.0 T magnetic resonance imaging. Mov Disord. 2011; 26:713–718. [PubMed: 21506148]

Christoforidis GA, Bourekas EC, Baujan M, Abduljalil AM, Kangarlu A, Spigos DG, Chakeres DW, Robitaille PM. High resolution MRI of the deep brain vascular anatomy at 8 Tesla: susceptibility-based enhancement of the venous structures. J Comput Assist Tomogr. 1999; 23:857–866. [PubMed: 10589559]

de Zwart JA, Ledden PJ, Kellman P, van Gelderen P, Duyn JH. Design of a SENSE-optimized high-sensitivity MRI receive coil for brain imaging. Magn Reson Med. 2002a; 47:1218–1227. [PubMed: 12111969]

de Zwart JA, van Gelderen P, Kellman P, Duyn JH. Application of sensitivity-encoded echo-planar imaging for blood oxygen level-dependent functional brain imaging. Magn Reson Med. 2002b; 48:1011–1020. [PubMed: 12465111]

de Zwart JA, Ledden PJ, van Gelderen P, Bodurka J, Chu R, Duyn JH. Signal-to-noise ratio and parallel imaging performance of a 16-channel receive-only brain coil array at 3.0 Tesla. Magn Reson Med. 2004; 51:22–26. [PubMed: 14705041]

de Zwart JA, Gelderen P, Fukunaga M, Duyn JH. Reducing correlated noise in fMRI data. Magn Reson Med. 2008; 59:939–945. [PubMed: 18383291]

Deelchand DK, Van de Moortele PF, Adriany G, Iltis I, Andersen P, Strupp JP, Vaughan JT, Ugurbil K, Henry PG. In vivo 1H NMR spectroscopy of the human brain at 9.4 T: initial results. J Magn Reson. 2010; 206:74–80. [PubMed: 20598925]

Deistung A, Rauscher A, Sedlacik J, Stadler J, Witoszynskyj S, Reichenbach JR. Susceptibility weighted imaging at ultra high magnetic field strengths: theoretical considerations and experimental results. Magn Reson Med. 2008; 60:1155–1168. [PubMed: 18956467]

Donahue MJ, Hoogduin H, van Zijl PC, Jezzard P, Luijten PR, Hendrikse J. Blood oxygenation level-dependent (BOLD) total and extravascular signal changes and DeltaR2* in human visual cortex at 1.5, 3.0 and 7.0 T. NMR Biomed. 2011; 24:25–34. [PubMed: 21259367]

Duong TQ, Kim DS, Ugurbil K, Kim SG. Localized cerebral blood flow response at submillimeter columnar resolution. Proc Natl Acad Sci U S A. 2001; 98:10904–10909. [PubMed: 11526212]

Duyn JH, van Gelderen P, Li TQ, de Zwart JA, Koretsky AP, Fukunaga M. High-field MRI of brain cortical substructure based on signal phase. Proc Natl Acad Sci U S A. 2007; 104:11796–11801. [PubMed: 17586684]

Flint JJ, Lee CH, Hansen B, Fey M, Schmidig D, Bui JD, King MA, Vestergaard-Poulsen P, Blackband SJ. Magnetic resonance microscopy of mammalian neurons. NeuroImage. 2009; 46:1037–1040. [PubMed: 19286461]

Fox MD, Raichle ME. Spontaneous fluctuations in brain activity observed with functional magnetic resonance imaging. Nat Rev Neurosci. 2007; 8:700–711. [PubMed: 17704812]

Fox MD, Snyder AZ, Vincent JL, Raichle ME. Intrinsic fluctuations within cortical systems account for intertrial variability in human behavior. Neuron. 2007; 56:171–184. [PubMed: 17920023]

Fukunaga M, Li TQ, van Gelderen P, de Zwart JA, Shmueli K, Yao B, Lee J, Maric D, Aronova MA, Zhang G, Leapman RD, Schenck JF, Merkle H, Duyn JH. Layer-specific variation of iron content in cerebral cortex as a source of MRI contrast. Proc Natl Acad Sci U S A. 2010a; 107:3834–3839. [PubMed: 20133720]

Fukunaga M, Li TQ, van Gelderen P, de Zwart JA, Shmueli K, Yao B, Lee J, Maric D, Aronova MA, Zhang G, Leapman RD, Schenck JF, Merkle H, Duyn JH. Layer-specific variation of iron content in cerebral cortex as a source of MRI contrast. Proc Natl Acad Sci U S A. 2010b; 107:3834–3839. [PubMed: 20133720]

Ge Y, Zohrabian VM, Grossman RI. Seven-Tesla magnetic resonance imaging: new vision of microvascular abnormalities in multiple sclerosis. Arch Neurol. 2008; 65:812–816. [PubMed: 18541803]

Glover PM, Cavin I, Qian W, Bowtell R, Gowland PA. Magnetic-field-induced vertigo: a theoretical and experimental investigation. Bioelectromagnetics. 2007; 28:349–361. [PubMed: 17427890]

Grohn HI, Michaeli S, Garwood M, Kauppinen RA, Grohn OH. Quantitative T(1rho) and adiabatic Carr-Purcell T2 magnetic resonance imaging of human occipital lobe at 4 T. Magn Reson Med. 2005; 54:14–19. [PubMed: 15968651]

Han SH, Song YK, Cho FH, Ryu S, Cho G, Song YQ, Cho H. Magnetic field anisotropy based MR tractography. J Magn Reson. 2011; 212(2):386–393. [PubMed: 21875818]

Haris M, Cai K, Singh A, Hariharan H, Reddy R. In vivo mapping of brain myo-inositol. NeuroImage. 2011; 54:2079–2085. [PubMed: 20951217]

He X, Yablonskiy DA. Biophysical mechanisms of phase contrast in gradient echo MRI. Proc Natl Acad Sci U S A. 2009; 106:13558–13563. [PubMed: 19628691]

Henry TR, Chupin M, Lehericy S, Strupp JP, Sikora MA, Sha ZY, Ugurbil K, Van de Moortele PF. Hippocampal sclerosis in temporal lobe epilepsy: findings at 7 T. Radiology. 2011; 261 (1):199–209. [PubMed: 21746814]

Hwang D, Kim DH, Du YP. In vivo multi-slice mapping of myelin water content using T2* decay. NeuroImage. 2010; 52:198–204. [PubMed: 20398770]

Hyde JS, Biswal BB, Jesmanowicz A. High-resolution fMRI using multislice partial k-space GR-EPI with cubic voxels. Magn Reson Med. 2001; 46:114–125. [PubMed: 11443717]

Kang CK, Park CA, Park CW, Lee YB, Cho ZH, Kim YB. Lenticulostriate arteries in chronic stroke patients visualised by 7 T magnetic resonance angiography. Int J Stroke. 2010; 5:374–380. [PubMed: 20854620]

Kerchner GA, Hess CP, Hammond-Rosenbluth KE, Xu D, Rabinovici GD, Kelley DA, Vigneron DB, Nelson SJ, Miller BL. Hippocampal CA1 apical neuropil atrophy in mild Alzheimer disease visualized with 7-T MRI. Neurology. 2010; 75:1381–1387. [PubMed: 20938031]

Kim T, Kim SG. Cortical layer-dependent arterial blood volume changes: improved spatial specificity relative to BOLD fMRI. NeuroImage. 2010; 49:1340–1349. [PubMed: 19800013]

Kim DS, Duong TQ, Kim SG. High-resolution mapping of iso-orientation columns by fMRI. Nat Neurosci. 2000; 3:164–169. [PubMed: 10649572]

Kollia K, Maderwald S, Putzki N, Schlamann M, Theysohn JM, Kraff O, Ladd ME, Forsting M, Wanke I. First clinical study on ultra-high-field MR imaging in patients with multiple sclerosis: comparison of 1.5 T and 7 T. AJNR Am J Neuroradiol. 2009; 30:699–702. [PubMed: 19147714]

Kominis IK, Kornack TW, Allred JC, Romalis MV. A subfemtotesla multi-channel atomic magnetometer. Nature. 2003; 422:596–599. [PubMed: 12686995]

Kruger G, Glover GH. Physiological noise in oxygenation-sensitive magnetic resonance imaging. Magn Reson Med. 2001; 46:631–637. [PubMed: 11590638]

Kwong KK, Belliveau JW, Chesler DA, Goldberg IE, Weisskoff RM, Poncelet BP, Kennedy DN, Hoppel BE, Cohen MS, Turner R, et al. Dynamic magnetic resonance imaging of human brain activity during primary sensory stimulation. Proc Natl Acad Sci U S A. 1992; 89:5675–5679. [PubMed: 1608978]

Langkammer C, Krebs N, Goessler W, Scheurer E, Yen K, Fazekas F, Ropele S. Susceptibility induced gray-white matter MRI contrast in the human brain. NeuroImage. 201110.1016/j.neuroimage.2011.08.045

Lee, D.; Hirano, Y.; Fukunaga, M.; Silva, AC.; Duyn, JH. Internat Soc for Magnetic Resonance in Medicine. Honolulu, Hawaii: 2009. Investigating the sources of phase contrast: iron oxide nanoparticle study to exclude deoxyhemoglobin as a major source of grey/white matter contrast; p. 1576

Lee J, Shmueli K, Fukunaga M, van Gelderen P, Merkle H, Silva AC, Duyn JH. Sensitivity of MRI resonance frequency to the orientation of brain tissue microstructure. Proc Natl Acad Sci U S A. 2010; 107:5130–5135. [PubMed: 20202922]

Lee J, van Gelderen P, Kuo LW, Merkle H, Silva AC, Duyn JH. T2*-based fiber orientation mapping. NeuroImage. 2011; 57:225–234. [PubMed: 21549203]

Lewis DA, Hashimoto T. Deciphering the disease process of schizophrenia: the contribution of cortical GABA neurons. Int Rev Neurobiol. 2007; 78:109–131. [PubMed: 17349859]

Li TQ, van Gelderen P, Merkle H, Talagala L, Koretsky AP, Duyn J. Extensive heterogeneity in white matter intensity in high-resolution T2*-weighted MRI of the human brain at 7.0 T. NeuroImage. 2006; 32:1032–1040. [PubMed: 16854600]

Li TQ, Yao B, van Gelderen P, Merkle H, Dodd S, Talagala L, Koretsky AP, Duyn J. Characterization of T(2)* heterogeneity in human brain white matter. Magn Reson Med. 2009; 62:1652–1657. [PubMed: 19859939]

Li W, Wu B, Liu C. Quantitative susceptibility mapping of human brain reflects spatial variation in tissue composition. NeuroImage. 2011; 55:1645–1656. [PubMed: 21224002]

Liu C. Susceptibility tensor imaging. Magn Reson Med. 2010; 63:1471–1477. [PubMed: 20512849]

Liu C, Li W, Johnson GA, Wu B. High-field (9.4 T) MRI of brain dysmyelination by quantitative mapping of magnetic susceptibility. NeuroImage. 2011a; 56:930–938. [PubMed: 21320606]

Liu C, Li W, Wu B, Jiang Y, Johnson GA. 3D fiber tractography with susceptibility tensor imaging. NeuroImage. 2011b

Macovski A. Noise in MRI. Magn Reson Med. 1996; 36:494–497. [PubMed: 8875425]

Madan N, Grant PE. New directions in clinical imaging of cortical dysplasias. Epilepsia. 2009; 50 (Suppl 9):9–18. [PubMed: 19761449]

Marenco S, Savostyanova AA, van der Veen JW, Geramita M, Stern A, Barnett AS, Kolachana B, Radulescu E, Zhang F, Callicott JH, Straub RE, Shen J, Weinberger DR. Genetic modulation of GABA levels in the anterior cingulate cortex by GAD1 and COMT. Neuropsychopharmacology. 2010; 35:1708–1717. [PubMed: 20357758]

Marques JP, Maddage R, Mlynarik V, Gruetter R. On the origin of the MR image phase contrast: an in vivo MR microscopy study of the rat brain at 14.1 T. NeuroImage. 2009; 46:345–352. [PubMed: 19254768]

Marques JP, van der Zwaag W, Granziera C, Krueger G, Gruetter R. Cerebellar cortical layers: in vivo visualization with structural high-field-strength MR imaging. Radiology. 2010; 254:942–948. [PubMed: 20177104]

Maze JR, Stanwix PL, Hodges JS, Hong S, Taylor JM, Cappellaro P, Jiang L, Dutt MV, Togan E, Zibrov AS, Yacoby A, Walsworth RL, Lukin MD. Nano-scale magnetic sensing with an individual electronic spin in diamond. Nature. 2008; 455:644–647. [PubMed: 18833275]

Muthukumaraswamy SD, Edden RA, Jones DK, Swettenham JB, Singh KD. Resting GABA concentration predicts peak gamma frequency and fMRI amplitude in response to visual stimulation in humans. Proc Natl Acad Sci U S A. 2009; 106:8356–8361. [PubMed: 19416820]

Ocali O, Atalar E. Ultimate intrinsic signal-to-noise ratio in MRI. Magn Reson Med. 1998; 39:462–473. [PubMed: 9498603]

Ogawa S, Lee TM. Magnetic resonance imaging of blood vessels at high fields: in vivo and in vitro measurements and image simulation. Magn Reson Med. 1990; 16:9–18. [PubMed: 2255240]

Ogawa S, Lee TM, Kay AR, Tank DW. Brain magnetic resonance imaging with contrast dependent on blood oxygenation. Proc Natl Acad Sci U S A. 1990; 87:9868–9872. [PubMed: 2124706]

Ogawa S, Tank DW, Menon R, Ellermann JM, Kim SG, Merkle H, Ugurbil K. Intrinsic signal changes accompanying sensory stimulation: functional brain mapping with magnetic resonance imaging. Proc Natl Acad Sci U S A. 1992; 89:5951–5955. [PubMed: 1631079]

Peters AM, Brookes MJ, Hoogenraad FG, Gowland PA, Francis ST, Morris PG, Bowtell R. T2* measurements in human brain at 1.5, 3 and 7 T. Magn Reson Imaging. 2007; 25:748–753. [PubMed: 17459640]

Petridou N, Wharton SJ, Lotfipour A, Gowland P, Bowtell R. Investigating the effect of blood susceptibility on phase contrast in the human brain. Neuro-Image. 2010; 50:491–498. [PubMed: 20026280]

Polimeni JR, Fischl B, Greve DN, Wald LL. Laminar analysis of 7 T BOLD using an imposed spatial activation pattern in human V1. NeuroImage. 2010; 52:1334–1346. [PubMed: 20460157]

Porter JR, Wright SM, Reykowski A. A 16-element phased-array head coil. Magn Reson Med. 1998; 40:272–279. [PubMed: 9702709]

Qiao H, Zhang X, Zhu XH, Du F, Chen W. In vivo 31P MRS of human brain at high/ultrahigh fields: a quantitative comparison of NMR detection sensitivity and spectral resolution between 4 T and 7 T. Magn Reson Imaging. 2006; 24:1281–1286. [PubMed: 17145398]

Qin L, van Gelderen P, Derbyshire JA, Jin F, Lee J, de Zwart JA, Tao Y, Duyn JH. Prospective head-movement correction for high-resolution MRI using an in-bore optical tracking system. Magn Reson Med. 2009; 62:924–934. [PubMed: 19526503]

Redpath TW. Signal-to-noise ratio in MRI. Br J Radiol. 1998; 71:704–707. [PubMed: 9771379]

Sanacora G, Mason GF, Rothman DL, Behar KL, Hyder F, Petroff OA, Berman RM, Charney DS, Krystal JH. Reduced cortical gamma-aminobutyric acid levels in depressed patients determined by proton magnetic resonance spectroscopy. Arch Gen Psychiatry. 1999; 56:1043–1047. [PubMed: 10565505]

Sati P, Silva AC, van Gelderen P, Gaitan MI, Wohler JE, Jacobson S, Duyn JH, Reich DS. In vivo quantification of T(2)() anisotropy in white matter fibers in marmoset monkeys. NeuroImage. 201110.1016/j.neuroimage.2011.08.064

Schweser F, Deistung A, Lehr BW, Reichenbach JR. Quantitative imaging of intrinsic magnetic tissue properties using MRI signal phase: an approach to in vivo brain iron metabolism? NeuroImage. 2011; 54:2789–2807. [PubMed: 21040794]

Seehafer JU, Kalthoff D, Farr TD, Wiedermann D, Hoehn M. No increase of the blood oxygenation level-dependent functional magnetic resonance imaging signal with higher field strength: implications for brain activation studies. J Neurosci. 2010; 30:5234–5241. [PubMed: 20392946]

Shapiro EM, Sharer K, Skrtic S, Koretsky AP. In vivo detection of single cells by MRI. Magn Reson Med. 2006; 55:242–249. [PubMed: 16416426]

Shmueli K, van Gelderen P, de Zwart JA, Horovitz SG, Fukunaga M, Jansma JM, Duyn JH. Low-frequency fluctuations in the cardiac rate as a source of variance in the resting-state fMRI BOLD signal. NeuroImage. 2007; 38:306–320. [PubMed: 17869543]

Silva AC, Koretsky AP. Laminar specificity of functional MRI onset times during somatosensory stimulation in rat. Proc Natl Acad Sci U S A. 2002; 99:15182–15187. [PubMed: 12407177]

Soellinger M, Rutz AK, Kozerke S, Boesiger P. 3D cine displacement-encoded MRI of pulsatile brain motion. Magn Reson Med. 2009; 61:153–162. [PubMed: 19097224]

Solano-Castiella E, Schafer A, Reimer E, Turke E, Proger T, Lohmann G, Trampel R, Turner R. Parcellation of human amygdala in vivo using ultra high field structural MRI. NeuroImage. 2011; 58 (3):741–748. [PubMed: 21726652]

Sumner P, Edden RA, Bompas A, Evans CJ, Singh KD. More GABA, less distraction: a neurochemical predictor of motor decision speed. Nat Neurosci. 2010; 13:825–827. [PubMed: 20512136]

Tallantyre EC, Morgan PS, Dixon JE, Al-Radaideh A, Brookes MJ, Morris PG, Evangelou N. 3 Tesla and 7 Tesla MRI of multiple sclerosis cortical lesions. J Magn Reson Imaging. 2010; 32:971–977. [PubMed: 20882628]

Thomas BP, Welch EB, Niederhauser BD, Whetsell WO Jr, Anderson AW, Gore JC, Avison MJ, Creasy JL. High-resolution 7 T MRI of the human hippocampus in vivo. J Magn Reson Imaging. 2008; 28:1266–1272. [PubMed: 18972336]

Thulborn KR, Waterton JC, Styles P, Radda GK. Rapid measurement of blood oxygenation and flow by high field NMR. NMR Biochem Soc Trans. 1981; 9:233.

Tkac I, Andersen P, Adriany G, Merkle H, Ugurbil K, Gruetter R. In vivo 1H NMR spectroscopy of the human brain at 7 T. Magn Reson Med. 2001; 46:451–456. [PubMed: 11550235]

Triantafyllou C, Hoge RD, Krueger G, Wiggins CJ, Potthast A, Wiggins GC, Wald LL. Comparison of physiological noise at 1.5 T, 3 T and 7 T and optimization of fMRI acquisition parameters. NeuroImage. 2005; 26:243–250. [PubMed: 15862224]

Triantafyllou C, Polimeni JR, Wald LL. Physiological noise and signal-to-noise ratio in fMRI with multi-channel array coils. NeuroImage. 2011; 55:597–606. [PubMed: 21167946]

Turner R, Jezzard P, Wen H, Kwong KK, Le Bihan D, Zeffiro T, Balaban RS. Functional mapping of the human visual cortex at 4 and 1.5 Tesla using deoxygenation contrast EPI. Magn Reson Med. 1993; 29:277–279. [PubMed: 8429797]

Ugurbil K, Hu X, Chen W, Zhu XH, Kim SG, Georgopoulos A. Functional mapping in the human brain using high magnetic fields. Philos Trans R Soc Lond B Biol Sci. 1999; 354:1195–1213. [PubMed: 10466146]

Uludag K, Muller-Bierl B, Ugurbil K. An integrative model for neuronal activity-induced signal changes for gradient and spin echo functional imaging. NeuroImage. 2009; 48:150–165. [PubMed: 19481163]

van Gelderen P, de Zwart JA, Lee J, Sati P, Reich D, Duyn JH. Nonexponential T2* decay in white matter. Mag Res Med. 201110.1002/mrm.22990

Ward HA, Riederer SJ, Grimm RC, Ehman RL, Felmlee JP, Jack CR Jr. Prospective multiaxial motion correction for fMRI. Magn Reson Med. 2000; 43:459–469. [PubMed: 10725890]

Weiger M, Schmidig D, Denoth S, Massin C, Vincent F, Schenkel M, Fey M. NMR Microscopy with isotropic resolution of 3.0 mum using dedicated hardware and optimized methods. Concepts Magn Reson B Magn Reson Eng. 2008; 33B:84–93.

Wiggins GC, Triantafyllou C, Potthast A, Reykowski A, Nittka M, Wald LL. 32-channel 3 Tesla receive-only phased-array head coil with soccer-ball element geometry. Magn Reson Med. 2006; 56:216–223. [PubMed: 16767762]

Wiggins GC, Polimeni JR, Potthast A, Schmitt M, Alagappan V, Wald LL. 96-Channel receive-only head coil for 3 Tesla: design optimization and evaluation. Magn Reson Med. 2009; 62:754–762. [PubMed: 19623621]

Wong CG, Bottiglieri T, Snead OC III. GABA, gamma-hydroxybutyric acid, and neurological disease. Ann Neurol. 2003; 54(Suppl 6):S3–S12. [PubMed: 12891648]

Yacoub E, Harel N, Ugurbil K. High-field fMRI unveils orientation columns in humans. Proc Natl Acad Sci U S A. 2008; 105:10607–10612. [PubMed: 18641121]

Yao B, Li TQ, Gelderen P, Shmueli K, de Zwart JA, Duyn JH. Susceptibility contrast in high field MRI of human brain as a function of tissue iron content. NeuroImage. 2009; 44:1259–1266. [PubMed: 19027861]

Yu X, Glen D, Wang S, Dodd S, Hirano Y, Saad Z, Reynolds R, Silva AC, Koretsky AP. Direct imaging of macrovascular and microvascular contributions to BOLD fMRI in layers IV–V of the rat whisker-barrel cortex. NeuroImage. 201110.1016/j.neuroimage.2011.08.001

Zhang K, Sejnowski TJ. A universal scaling law between gray matter and white matter of cerebral cortex. Proc Natl Acad Sci U S A. 2000; 97:5621–5626. [PubMed: 10792049]

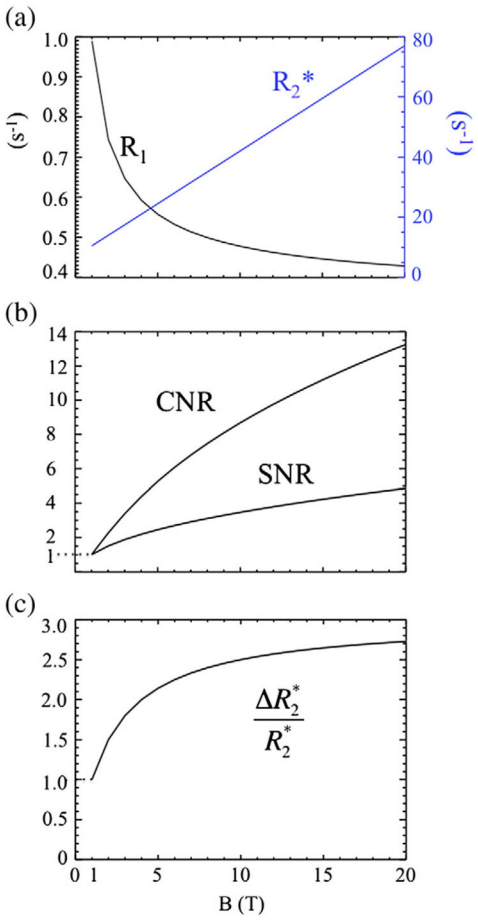

Fig. 1.

Dependence of relaxation rates, SNR, and CNR on field strength *B*. (a) relaxation rate R_1 and R_2^* as function of field strength according to Eqs. (1a) and (1b) respectively. (b) SNR and CNR as function of *B*. CNR increases faster than SNR by a factor $\Delta R_2^*/R_2^*$, which is graphed in (c). Both tend to a square root dependency on *B* in the high field limit. Quantities in (b) and (c) are normalized to the values at *B*=1 T.